Submitted for inclusion in: Remote Sensing of Environment and Forest Management (A. Mehrotra and R. K. Suri, Eds.)

PASSIVE MICROWAVE REMOTE SENSING FOR LAND RESOURCES

Eni G. Njoku
Jet Propulsion Laboratory
California Institute of Technology
Pasadena, CA 91109

SUMMARY

Spaceborne microwave radiometry is an important technique for obtaining global estimates of parameters important to the Earth's hydrologic cycle, land resources, environmental monitoring, and climate. They key physical processes involved in these applications are the land-atmosphere exchanges of heat and moisture, and their status and variability on different time and space scales. Microwave observations are sensitive to geophysical parameters that influence these processes, such as surface temperature, soil moisture, and vegetation parameters which influence transpiration. Microwave radiometry from space using current sensors is limited to spatial resolutions of -10 to 120 km, depending on wavelength. These resolutions are adequate for climate and large-scale monitoring applications. Future spaceborne sensors currently in the development stage will have better spatial resolutions, more appropriate for mesoscale monitoring, weather, and hydrologic applications. Radiative transfer models have been developed to describe the effects of land surface and atmospheric parameters on microwave brightness temperature. These models have been used to interpret satellite observations at a range of frequencies from 1,4 to 90 GHz using observations from spaceborne sensors such as the Nimbus-7 SMMR and DMSP SSM/I. Estimates of surface parameters from satellite data include vegetation index and seasonal flooding derived from the 37 GHz channels of the SMMR and SSM/I instruments, and soil moisture, temperature, and vegetation change derived from multiple channels of the same instruments. The effects of atmospheric humidity and clouds on surface estimates using the higher frequency channels have also been studied. Results show that spaceborne radiometers can provide information of critical importance in such operational applications as agriculture, water resource planning, flood and drought monitoring, and weather and climate forecasting.

Keywords: Microwave, radiometry, hydrology, land resources

I. INTRODUCTION

Microwave radiometers have observed the Earth from space since the late 1960's (Njoku, 1982; Hollinger et al., 1990). Since then most applications have emphasized observations of the atmosphere, oceans, and polar regions. Interpretation of microwave observations over land (e.g. for monitoring soil moisture, vegetation, temperature, and precipitation) has not been emphasized due to the low spatial resolution of microwave radiometers relative to the spatial scales of land surface features, and to the complexity in modeling the radiative emission and transfer characteristics of land surfaces. In recent years, however, improved models have been developed describing the relationships between brightness temperature and land surface parameters over a range of frequencies, polarizations, and viewing angles. It has been recognized that microwave techniques permit unique observations of land surface parameters critical to the Earth's hydrologic cycle, such as soil moisture, vegetation, precipitation, and snow, Increasing amounts of global, multiyear data have been acquired from spaceborne radiometers such as the SMMR on the Nimbus-7 satellite and the SSM/I on the DMSP satellites, and there is now an awareness of the need for quantitative estimation of land surface parameters over large spatial and temporal scales for environmental monitoring and as boundary conditions for validation of regional and global climate models (Becker et al., 1988; GEWEX, 1990). These developments have led to increased interest in the potential of microwave radiometry for global observations of land surfaces.

Figure 1 shows the major processes taking place in the Earth's hydrologic cycle. Precipitation in the form of rain is partitioned at the surface into infiltration, runoff, and evaporation. Infiltration results in groundwater flow and soil water storage, some of which (in the root zone) is available to plants and re-enters the atmosphere by transpiration, Precipitation in the form of snow results in storage followed by snowmelt and further infiltration and runoff. If

precipitation is excessive and the soil is near saturation flooding may occur. Conversely, if precipitation is minimal overextended periods, and the water storages are depleted, this may lead to drought conditions. It is clear that understanding and monitoring the spatial and temporal variability of these aspects of the hydrologic cycle is critical to managing the water supply for agricultural, industrial, and domestic needs. The processes of evaporation and transpiration (evapotranspiration) are associated with transfer of latent heat from the surface into the atmosphere. The latent heat flux is a component of the surface energy balance (other components are net radiation, sensible heat flux, and soil heat flux) and is an important process in determining regional and global weather and climate patterns (Miller, 1977). General circulation model (GCM) simulations have shown that soil moisture conditions area critical factor in determining regional and global climate (e.g Shukla and Mintz, 1982).

Land-atmosphere interaction models used in these GCM simulations seek to describe the exchanges of energy and water between the surface and atmosphere in terms of physically measurable parameters (Sellers et al,, 1986). Some of these parameters such as incoming solar radiation, surface albedo, soil moisture, vegetation type and fractional cover, surface temperature, snow cover, precipitation, and others can be measured by a combination of remote sensing techniques including visible, infrared, and active and passive microwave. Most of these parameters are amenable to direct measurement using microwave radiometry. In practice a combination of remote sensing data and surface meteorological data are needed as inputs to the surface flux models since no single approach can adequately provide estimates of all the required inputs (Kustas et al., 1991),

In this paper we discuss the status of spaceborne microwave remote sensing for land applications. The discussion is restricted, due to space limitations, to snow-free land, in particular to measurements of soil moisture, temperature, and vegetation.

II. PASSIVE MICROWAVE SENSING

In order to illustrate the applications of microwave radiometry in land remote sensing a short description of the radiative transfer models and estimation techniques is presented. More detailed descriptions are available in Ulaby et al. (1986) and Tsang et al. (1985). Radiative transfer models relate brightness temperatures measured by a spaceborne radiometer to physical features of the surface and atmosphere, The physical features are described by parameters which govern the absorption, emission, and scattering properties of the medium, The relationship of these parameters to the measured brightness temperatures maybe expressed as:

$$T_{B_i} = F_i(\bar{p}) \tag{1}$$

where, T_{Bi} are brightness temperatures at wavelengths (or channels) i, and F_i are radiative transfer functions of geophysical parameters p_j (which make up the parameter vector $\bar{p}$). information on the parameters p_j may be extracted from the satellite measurements T_{Bi} via an inversion model:

$$p_j = G_j(\bar{T}_B) \tag{2}$$

where, Gj are inverse relationships derived from F_i and may include a priori information or constraints. If the number of measurements T_{Bi} making up the brightness temperature vector $\bar{T}_B$ is smaller than the number of parameters p_j then the inverse problem is underdetermined and additional information or constraints must be applied to solve for p_j. In some cases the relationships of Equation (1) are nonlinear and an inversion technique based on Equation (2) must be applied iteratively to converge to the correct solution,

The number of parameters required to accurately describe a given surface and atmosphere for a range of environmental conditions can be quite large (Sellers et al., 1986), and may include parameters for which information is not primarily of interest. Hence the goal is often to simplify the models to parameters of direct interest, while adequately describing the physics, and to provide a priori information (and associated uncertainties) for the remaining parameters, For spaceborne applications it is particularly important to use simple parameterizations since the number of radiometer measurement channels is limited, and it is often difficult to get adequate a priori information from other sources (i.e. climatology or ground truth), With simple parameterizations it is possible to validate the models of Equation (1) using satellite data, and to develop inversion algorithms based on the form of Equation (2) to retrieve surface parameter values from the satellite data,

For snow-free land, the surface terrain and radiometer viewing configuration can be depicted schematically as in Figure 2. A radiative transfer model simulating this configuration, which has been adopted by several investigators (e.g. Mo et al., 1982; Kerr and Njoku, 1990; Choudhury et al., 1990), is that of a single uniform vegetation layer above a rough soil surface. The soil is assumed to have uniform vertical distribution of moisture and temperature. Above the surface is an atmosphere with mean temperature T_a, and opacity τ_a. The radiative transfer equation at a given frequency for this model can be expressed as:

$$T_{B_p} = T_a (1 - e^{-\%}) [1 + r_{s_p} e^{-(\% + 2\tau_c)}] + T_e e^{-\%} [1 - r_{s_p} e^{-2\tau_c}] \qquad (3)$$

where, r_{s_p} is the reflectivity of the soil (beneath the vegetation canopy), τ_c is the canopy opacity, and T_e *is* the effective temperature of the soil surface and vegetation (here assumed equal). The subscript p denotes polarization (vertical v, or horizontal h). In this expression rough surface scattering is approximated by a modified specular reflectivity r_{s_p}. The reflectivity depends on the soil moisture m, and therms height σ and horizontal correlation length *1* of the surface roughness

(Tsang et al., 1985). It is assumed for simplicity that the vegetation is comprised of sparse, randomly distributed absorbers, with no scattering within the medium or reflection at the air-vegetation interface. The opacity τ_c is then a function of the vegetation water content W_c and a factor u which varies according to the canopy geometry (as determined by vegetation type) (Kirdyashev et al., 1979). Equation (3) assumes that at the frequencies of concern (surface-viewing, atmospheric window frequencies) the atmosphere is not highly absorbing and can be described adequately by a mean temperature approximation (Westwater et al., 1990). The atmospheric opacity τ_a is a function of the atmospheric columnar water vapor V, and cloud liquid water content L. Thus, for this simple model Equation (3) has the form of Equation (1) where the parameter vector $\bar{p}$ has the components:

$$\bar{p} = [m, \sigma, 1, W_c, u, T_e, T_a, V, L] \qquad (4)$$

More sophisticated models take into account the following factors. The non-scattering assumption becomes inaccurate for most types of vegetation at frequencies above ~10 GHz. At higher frequencies Equation (3) can be modified to include single and higher orders of scattering (Tsang et al., 1985). Expressions for opacity τ_c and scattering phase function $P(\theta,\theta')$ have been developed to take into account scattering from leaves, branches, and stems in the vegetation layer (Mo et al., 1982; Choudhury et al., 1990; Chuang et al., 1980), For moderate scattering, the single scattering albedo @(the ratio of absorption to extinction coefficients) is a useful parameter. Its effect is generally to reduce the brightness temperature of the vegetation canopy, At frequencies greater than ~10 GHz, ω may become significant for certain types of vegetation, and may exhibit a polarization dependence due to preferred orientations of leaves and stalks in the medium, In some cases this can lead to unexpectedly lower values for vertical than for horizontal polarizations in observed canopy brightness temperatures (Mätzler, 1990), For a radiometer footprint which includes regions of bare and vegetated soil, the brightness temperature may be modeled as a composite quantity:

$$T^{*}_{B_p} = c\, T_{B_{p,can}} + (1 - c)\, T_{B_{p,bare}} \qquad (5)$$

where, C is the canopy fractional coverage, and:

$$T_{B_{p\ can}} = T_{B_p}\ ; \qquad \text{(Equation (3), where: } T_e = T_{e_1}\text{)} \qquad (6a)$$

$$T_{B_{p,bare}} = T_{B_p}\ ; \qquad \text{(Equation (3), where: } \tau_c = \text{O; } T_e = T_{e_2}\text{)} \qquad (6b)$$

and, *Tel* and T_{e2} are the temperatures of the vegetation-covered and bare soil, respectively. *Tel* and T_{e2} may differ significantly due to the different surface heat flux conditions in the two cases.

Observational data can be used to illustrate some of the relationships between brightness temperature and geophysical parameters expressed by Equations (1), (3), and (4). For example, Figure 3 shows aircraft radiometer measurements of brightness temperature T_B at a wavelength of 21 cm (f = 1.4 GHz) as a function of soil moisture m (Schmugge, 1990). Independent measurements of σ and *1* were not made, **but** the test sites could be grouped into three roughness categories based on ground photographs. A linear relationship of the form: T_B = a + b m is observed, where a and b are coefficients which depend on the degree of roughness. The effects of roughness observed in Figure 3 for these agricultural fields is not large at this wavelength. The linear relationships may thus be inverted to obtain useful estimates of soil moisture from the brightness temperature data. The scatter observed in the data maybe due to variations in other parameters such as surface temperature, or to errors in either the brightness temperature or soil moisture measurements,

Polarization Indices

At off-nadir angles (such as the ~50° viewing angle of the SMMR and SSM/I instruments - see Table 1) the vertical and horizontal brightness temperatures exhibit different functional dependencies on surface moisture, roughness, and vegetation parameters. Bare, smooth soils with high moisture contents exhibit large differences between T_{Bv} and T_{Bh}, while dry soils, increased surface roughness, and vegetation all tend to decrease the polarization difference. For this reason, indices representing the polarization difference have been used to interpret satellite data, Two such indices are the Microwave Polarization Difference Temperature (MPDT, or AT) (Choudhury, 1989) and the Polarization Ratio, or Index (PR, or PI) (Kerr and Njoku, 1990; Wang et al., 1982; Paloscia and Pampaloni, 1988). These are defined as:

$$AT = T_{B_v} - T_{B_h} \tag{7a}$$

$$PR = (T_{B_v} - T_{B_h}) / (T_{B_v} + T_{B_h}) \tag{7b}$$

When atmospheric absorption is negligible, the indices take the simple forms:

$$AT = T_e (\varepsilon_v - \varepsilon_h) \tag{8a}$$

$$PR = (\varepsilon_v - q)/ (\varepsilon_v + \varepsilon_h) \tag{8b}$$

where, $\varepsilon_p = 1 - r_{s_p} e^{-2\tau_c}$ (p = v or h) is the emissivity of the composite soil/vegetation surface. *AT* and *PR* have similar sensitivities to moisture, roughness, and vegetation. However *PR is* independent of surface temperature and hence can be used to study moisture and vegetation "effects without considering temperature variability. Figure 4 shows the simulated variation of *AT* with frequency using representative values of model parameters. The baseline curve is for values of T_e = 15 "C, m = 0.3 g/cm^2, $\sigma = W_c = V = L = O$, and C = 0.3. The remaining curves show the effects of cumulatively changing the parameters in the sequence: T_e = 25 "C, m = 0.05

g/cm^2, σ = 0.05 cm, WC= $0.1 kg/m^2$, $v = 4.5\ g/cm^2$, L = 0,1 g/cm^2. For example, the bottom curve is for all parameters changed to the above values, The main features to be observed from Figure 4 are the large increase in *AT* with increased moisture, and the decrease in *AT* with increasing vegetation, roughness, and atmospheric moisture, especially at the higher frequencies. The magnitude of these effects varies with frequency, hence, in principle, multifrequency measurements may be used to independently estimate the geophysical parameters. The frequencies of the Nimbus-7 Scanning Multichannel Microwave Radiometer (SMMR) (Tabld) are indicated on the figure for reference.

111. SPACEBORNE OBSERVATIONS ANI) APPLICATIONS

Table 1 lists the primary spaceborne microwave radiometers for which land applications studies have been reported in the literature. Descriptions of the first five instruments may be found in Njoku (1982) and Hollinger et al. (1990). Table 1 also includes two sensors which are currently in the approved (MIMR) and planning (ESTAR) stages. These instruments are described in ESA (1990) and LeVine et al. (1990), respectively.

Land Cover Classification

Studies using data from the Nimbus-7 SMMR and the DMSP SSM/I have been used to classify land cover types. Townshend et al, (1989) compared SMMR 37 GHz MPDT data with Normalized Difference Vegetation Index (NDVI) data derived from the AVHRR instrument on the NOAA satellites (visible and infrared channels). The multi-temporal characteristics of the data over an annual cycle were used with a rnaximum-likelihood technique to classify up to sixteen land cover types in Africa and South America. The accuracy with which the classifier correctly identified the classes is shown in Figure 5 for a few selected classes. The 37 GHz SMMR data showed a high degree of success (>80%; and higher success than the AVHRR) in

Table 1: Spaceborne microwave radiometers used for land studies.

SENSOR (Satellite)	Year of Launch.	FREQUENCIES (GHz) (Approx. Spatial Resolution (km))						
ESMR-5 (Nimbus-5)	1972				19.3 (25)			
S-194 (Skylab)	1973	1.4 (115)						
ESMR-6 (Nimbus-6)	1975						37.0 (25)	
SMMR (Nimbus-7)	1978		6.6 (140)	10.7 (90)	18.0 (55)	21.0 (45)	37.0 *(30)*	
SSM/I (DMSP)	1987				19.3 (70)	22.2 (60)	37.0 (37)	85. S (15)
MIMR/AMSR (EOS)	1998(?)		6.8 (60)	10.7 (38)	18.7 (22)	23.8 (20)	36.5 (12)	90 (5)
ESTAR (??)	(?)	1.4 (10)						

classifying land cover in the arid zones (i.e. desert, semi-desert, Sahel, and Northern Sudan). Less accuracy than the AVHRR was found in regions of denser vegetation. This indicates the high sensitivity at 37 GHz to small amounts of vegetation, and the lower sensitivity at high vegetation opacities. Better accuracy in classifying denser vegetation may be attainable using lower SMMR frequencies (hence lower opacities), although degraded spatial resolution results. Classification studies using multifrequency SMMR and SSM/I data have also been reported by Ferraro et al. (1986), Neale et al, (1990), and others, These studies have derived empirical combinations of radiometer channels sensitive to specific surface types, yet these results often do not provide sufficient insight into the physical interactions necessary to develop quantitative parameter retrieval algorithms.

Soil Moisture and Flooding

A number of case studies have been performed for estimating soil moisture or wetness using spaceborne microwave data, These date from early sensors such as the L-band radiometer on Skylab to the more recent SMMR and SSM/I. Because of the low spatial resolution (-100 km) at the L- to C-band frequencies, which are most useful for soil moisture sensing due to their increased vegetation penetration, it is difficult to obtain representative ground truth data for comparison with the spaceborne data over similar spatial scales. Much use has been made therefore of the Antecedent Precipitation Index (API) which combines sparsely sampled soil moisture measurements with meteorological data and water balance models to generate a large-scale area-averaged moisture index. McFarland (1976) showed a strong relationship between the Skylab 21-cm brightness temperatures and Antecedent Precipitation Index (API) for data obtained over the central U.S. A correlation coefficient of greater than 0.85 was found between brightness temperature and API. Eagleman and Lin (1976) performed a similar analysis comparing the brightness temperature with soil moisture estimates based on a combination of actual ground measurements and calculations of the soil moisture using a climatic water balance model,

Studies using Nimbus-5 Electrically Scanning Microwave Radiometer (ESMR) 1.55-cm wavelength data (Schmugge et al., 1977) indicated the limitations on soil moisture sensing at this wavelength due to the increased sensitivity to vegetation. Wang (1985) investigated the vegetation sensitivity by analysis of Skylab 21-cm radiometer data and Nimbus-7 SMMR 5-cm data, The microwave brightness temperatures were correlated to API but there was a strong dependence on vegetation cover at the shorter wavelength. These studies point out the need for information on the surface vegetation cover before inferences of soil moisture can be made from satellite observations over vegetated terrain.

Choudhuryand Golus (1988) investigated the useofan AVHRR-derived vegetation index (NDVI) to quantify the vegetation effects on microwave soil moisture, Figure 6 illustrates the relationship between Nimbus-7 SMMR 6 GHz horizontally polarized data and API for two regions in eastern Kansas and in western Texas. The Kansas site was more vegetated than the Texas site as indicated by NDVI values of 0.4 and 0.25 respectively. The slope of the T_B *vs.* API regression was found to be correlated with NDVI, indicating that from satellite measurements of T_B and NDVI it may be possible to estimate API, Seasonal flooding of selected areas over South America has also been studied by Giddings and Choudhury (1989) using 37 GHz 25 km resolution data from the Nimbus-7 SMMR. Under certain conditions, an increase in river height can lead to flooding of the low-lying river banks and an increase in the area of exposed water. Although no precise relationship has been developed between river height, exposed water, and brightness temperature, the similarity of the observed river height and brightness temperature time series indicates the potential of passive microwave data for monitoring seasonal flooding.

Vegetation

The relationship between SMMR 37 GHz MPDT and vegetation characteristics has been studied by Choudhury (1989) and others. Observed temporal variations of MPDT for three regions over Africa are shown in Figure 7. These regions are the Sahara desert (Egypt), Sahel (Niger), and tropical savanna (Botswana). There is little vegetation over the Sahara region where the MPDT values are highest and show little temporal variation. Over the Sahel, as the annual grasses grow in response to rainfall, the MPDT values decrease and then increase as the grasses dry out and lose their moisture. The vegetation growth over the tropical savanna in the southern hemisphere is roughly six months out of phase with the northern hemisphere. The savanna vegetation has a woody component associated with the shrubs and trees, and the MPDT values

are somewhat smaller than over the Sahel. Figures 5 and 7 indicate the potential of SMMR data for monitoring temporal changes in vegetation density and extent of ecosystems in arid regions.

Kerr and Njoku (1990) used a model similar to that of Equations (3) and (4) to interpret multifrequency data from the Nimbus-7 SMMR over the African Sahel. Data were analyzed in terms of the polarization ratio (PR) at frequencies from 6.6 to 37 GHz, and showed that the temporal changes in PR over an annual cycle were consistent with local annual variations in meteorological and climatic conditions of the surface and atmosphere. This work, and more recent studies, have shown that data such as shown in Figure 7 must be interpreted with caution since corrections for seasonal variations of atmospheric moisture (water vapor and clouds) may be necessary.

Temperature

There have been few studies of the use of microwave radiometry in estimating land surface temperature. This has perhaps been due to the difficulty in accounting for the variability of surface emissivity, which must be estimated in order to retrieve surface temperature. It is also difficult to define a mean radiating temperature over the often complex terrain within a radiometer footprint, and to acquire representative in situ temperature measurements for validating the satellite measurements. McFarland et al. (1990) performed a regression analysis using DMSP SSM/I data which showed that by careful screening of surface types, and by matching multifrequency SSM/I data spatially and temporally with meteorological near-surface atmospheric temperatures, agreement between satellite and in situ temperature estimates could be obtained to ‘an rms accuracy of -2-3 ‘C. For most surfaces the 85 GHz vertical channel showed the best correlation with temperature (presumably since for this channel the surface has the least variable emissivity), and performed reasonably well as a temperature estimator when corrections for

atmospheric effects from the 22 and 37 GHz channels were available, Figure 8 shows the regression results for moist soil, and tabulated values for the other surface types.

IV. FUTURE WORK

The previous sections have described modeling and data analysis results that indicate the uses of passive microwave space observations for land applications. Future work will focus on development of more quantitative parameter retrieval algorithms and will make use of higher resolution multifrequency data, Multi-frequency, dual-polarized data will be necessary to retrieve multiple parameters such as temperature, soil moisture, and vegetation biomass. Stable instrument calibrations will be required to enable detection of changing land cover features on multiyear time-scales. Retrieval algorithms will need to account for nonlinear effects of vegetation biomass and fractional coverage on brightness temperature, and a means for correcting atmospheric effects at higher frequencies will be necessary, Use of microwave water vapor sounders operating at frequencies near 183 GHz may satisfy this latter requirement.

The requirement for multifrequency high resolution data will be addressed to some extent by the Multifrequency Imaging Microwave Radiometer (MIMR) to be launched on the Earth Observing System (EOS) in approximately the year 2000, and the Electrically Scanned Thinned Array Radiometer (ESTAR) currently in the early planning stage (Table 1). A focused program of ground-based and aircraft controlled field experiments is needed to improve the microwave models of vegetation emission and scattering and to develop retrieval algorithms in preparation for these new data sources.

V. ACKNOWLEDGMENT

This paper represents one phase of work carried out at the Jet Propulsion Laboratory, California Institute of Technology, under contract to the National Aeronautics and Space Administration.

VI. REFERENCES

Becker, F., H.-J. Belle, and P. R. Rowntree (1988): The International Satellite Land Surface Climatology Project (ISLSCP), *ISLSCP Report #10*, ISLSCP Secretariat, Berlin, FRG.

Choudhury, B. J. and R. E. Golus (1988): Estimating soil wetness using satellite data, *Int. J. Rem. Sens.*, *9, 1251-1257.*

Choudhury, B. J. (1989): Monitoring global land surface using Nimbus-7 37 GHz data. Theory and examples, *Int. J. Rem. Sens.*, *10, 1579-1605,*

Choudhury, B. J., J. R. Wang, A. Y. Hsu, and Y. L. Chien (1990): Simulated and observed 37 GHz emission over Africa, *Int. J. Rem. Sens.*, *11,* 1837-1868.

Chuang, S. L., J. A. Kong, and L. Tsang (1980): Radiative transfer theory for passive microwave remote sensing of a two-layer random medium with cylindrical structures, *J. Appl. Phys.*, *51, 5588-5593.*

Eagleman, J, R, and W. C. Lin (1976): Remote sensing of soil moisture by a 21 cm passive radiometer, *J. Geophys. Res.*, 81, #21.

ESA (1990): The Multifrequency Imaging Microwave Radiometer, Instrument Panel Report, *ESA SP-1138*, European Space Agency, Paris, France,

Ferraro, R, R., N, C. Grody, and J. A. Kogut (1986): Classification of geophysical parameters using passive microwave satellite measurements, *IEEE Trans. Geosci. Rem, Sens.*, *GE-24, 1008-1013.*

GEWEX (1990): Scientific plan for the Global Energy and Water Cycle Experiment, *Report #WCRP-40 (WMO/TD #376)*, World Meteorological Organization, Geneva, Switzerland.

Giddings, L. and B. J. Choudhury (1989): Observation of hydrological features with Nimbus-7 37 GHz data applied to South America, *Int. J. Rem. Sens.*, 10, 1673-1686.

Hollinger, J. P., J, L. Pierce, and G. A, Poe (1990): SSM/I instrument evaluation, *IEEE Trans. Geosci. Rem. Sens.*, *28, 781-790.*

Kerr, Y. H. and E. G, Njoku (1990): A semiempirical model for interpreting microwave emission from semiarid land surfaces as seen from space, *IEEE Trans. Geosci. Rem. Sens.*, *28, 384-393.*

Kirdyashev, K. P., A. A. Chukhlantsev, and A. M. Shutko (1979): Microwave radiation of the Earth's surface in the presence of a vegetation cover, *Radio Eng. Electron, Physics, 24,37-44.*

Kustas, W, P., D. C. Goodrich, M. S. Moran, and others (1991): An interdisciplinary field study of the energy and water fluxes in the atmosphere-biosphere system over semi-arid rangelands: Description and some preliminary results, *Bull. Am. Met, Soc., 72, 1683-1705.*

Le Vine, D. M., M. Kao, A. B. Tanner, C. T. Swift, and A. Griffis (1990): Initial results in the development of a synthetic aperture radiometer, *IEEE Trans. Geosci. Rem. Sens., 28,* 614-619.

Mätzler, C. (1990): Seasonal evolution of microwave radiation from an oat field, *Rem, Sens.* Env., 31, 161-173,

McFarland, M, J. (1976): The correlation of Skylab L-band brightness temperatures with antecedent precipitation, in: *Proc. NASA Earth Resources. Symp.*, NASA TMX-58 168.

McFarland, M. J., R. L. Miller, and C. M. U. Neale (1990): Land surface temperature derived from the SSM/I passive microwave brightness temperatures, *IEEE Trans. Geosci. Rem. Sens., 28, 839-845.*

Miller, D. H. (1977): *Water at the Surface of the Earth,* Academic Press, New York,

Mo, T., B, J. Choudhury, T. J. Schmugge, J, R. Wang, and T. J. Jackson (1982): A model for microwave emission from vegetation-covered fields, *J. Geophys. Res., 87,* 1122.9-11237,

Neale, C. M. U., M. J. McFarland, and K. Chang (1990): Land-surface-type classification using microwave brightness temperatures from the Special Sensor Microwave/Imager, *IEEE Trans. Geosci. Rem. Sens., 28, 829-838.*

Njoku, E. G. (1982): Passive microwave remote sensing of the Earth from space - A review, *Proc. IEEE, 70, 728-750,*

Paloscia, S, and P. Pampaloni (1988): Microwave polarization index for monitoring vegetation growth, *IEEE Trans. Geosci. Rem. Sens., 26, 617-621.*

Schmugge, T. J., J. M. Meneely, A. Rango, and R. Neff (1977): Satellite microwave observations of soil moisture variations, *Water Resources Bull., 13, 265-281.*

Schmugge, T. J. (1990): Measurements of surface soil moisture and temperature, in: *Remote Sensing of Biosphere Functioning* (R, J. Hobbs and H. A. Mooney, Eds), Ch 3, Springer-Verlag, New York, NY.

Sellers, P. J., Y. Mintz, Y. C, Sud, and A. Dalcher (1 986): A simple biosphere model (SiB) for use within general circulation models, *J. Arm. Sci., 43, 505-531.*

Shukla, J. and Y, Mintz (1982): Influence of land-surface evapotranspiration on the Earth's climate, *Science, 215, 1498-1500.*

Smagorinsky, J, (1982): Large scale climate modeling and small scale physical processes, in: *Land Surface Processes in Atmospheric General Circulation Models* (P. S. Eagleson, cd,), Cambridge University Press, New York, NY.

Townshend, J. R. G., C. O. Justice, B. J. Choudhury, C. J. Tucker, V. T. Kalb, and T. E. Goff (1989): A comparison of SMMR and AVHRR data for continental land cover characterization, *Int. J. Rem. Sens., 10, 1633-1642.*

Tsang, L., J. A. Kong, and R. T. Shin (1985): *Theory of Microwave Remote Sensing,* Wiley-Interscience, New York, NY.

Ulaby, F. T., R. K. Moore, and A. K. Fung (1986): *Microwave Remote Sensing, Vol. III: From Theory to Applications,* Artech House, Dedham, MA.

Wang, J. R., J. E. McMurtrey, E. T, Engman, and others (1982): Radiometric measurements over bare and vegetated fields at 1.4 GHz and 5 GHz frequencies, *Rem. Sens. Env., 12,* 295-311.

Wang, J. R. (1985): Effect of vegetation on soil moisture sensing observed from orbiting microwave radiometers, *Rem, Sens. Environ., 17,* 141-151.

Westwater, E. R., J. B. Snider, and M. J. Falls (1990): Ground-based radiometric observations of atmospheric emission and attenuation at 20.6, 31.65, and 90.0 GHz: A comparison of theory and measurements, *IEEE Trans. Ant, & Propagat., 38,* 1569-1580.

FIGURE CAPTIONS

Figure 1: Major processes involved in the Earth's hydrologic cycle (adapted from Smagorinsky, 1982),

Figure 2: Soil-vegetation configurations and radiometer viewing geometry (adapted from Sellers et al., 1986).

Figure 3: Plot of T_B versus soil moisture for aircraft observations at 21-cm wavelength over a test site in Hand Conty, South Dakota. The data are grouped into three roughness categories based on ground photographs (from Schmugge, 1990).

Figure 4: Variation of polarization difference ΔT with frequency for cumulative contributions of surface and atmospheric model parameters.

Figure 5: Classification accuracy for selected surface types in Africa using SMMR 37 GHz MPDT and AVHRR NDVI (from Townshend et al., 1989).

Figure 6: Comparison of SMMR 6.6 GHz brightness temperature with antecedent precipitation index (from Choudhury and Golus, 1988).

Figure 7: Temporal variations of SMMR 37 GHz MPDT in different vegetation zones (from Choudhury, 1989).

Figure 8: Land surface temperature regression estimates using SSM/I data and in situ screen air temperatures (from McFarland et al., 1990).

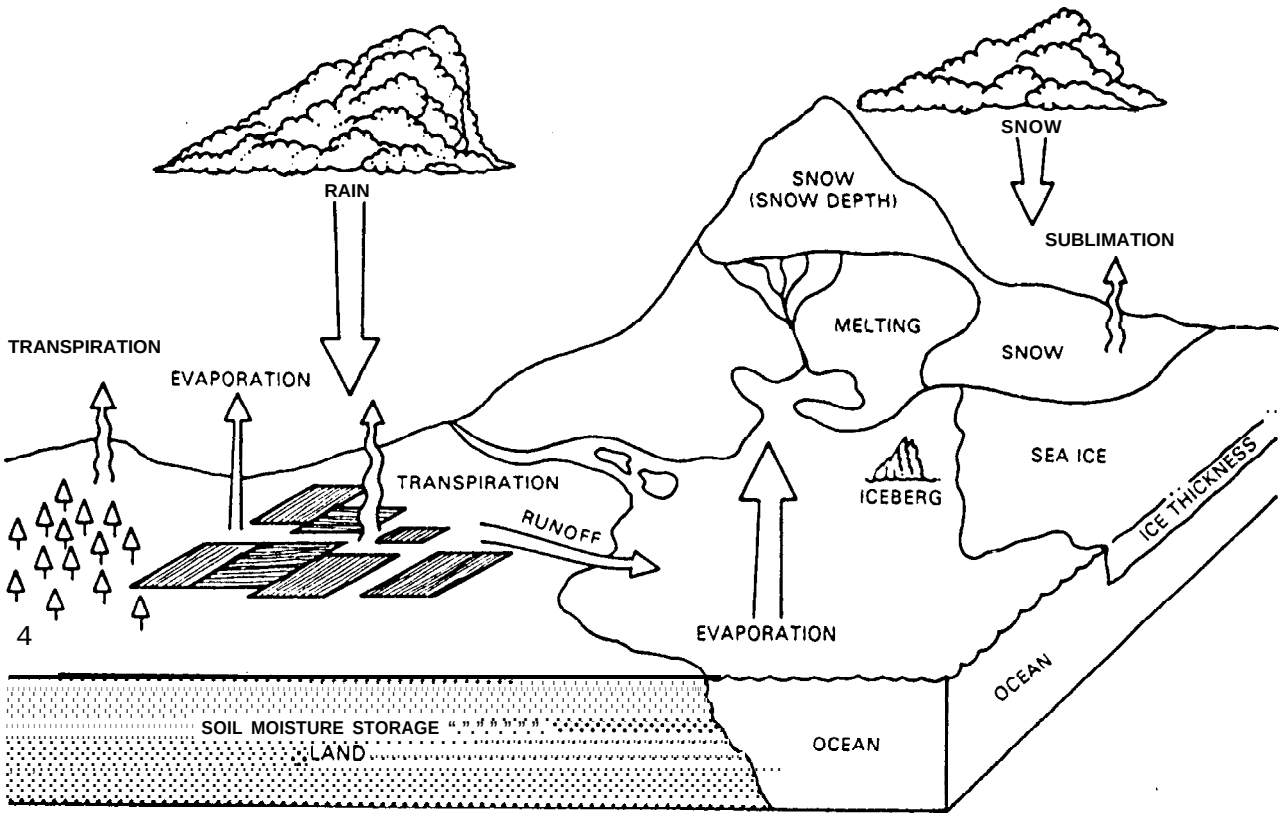
RAIN
SNOW
SNOW
(SNOW DEPTH)
SUBLIMATION
TRANSPIRATION
EVAPORATION
MELTING
SNOW
SEA ICE
ICEBERG
ICE THICKNESS
TRANSPIRATION
RUNOFF
EVAPORATION
OCEAN
SOIL MOISTURE STORAGE
LAND
OCEAN

Figure 1

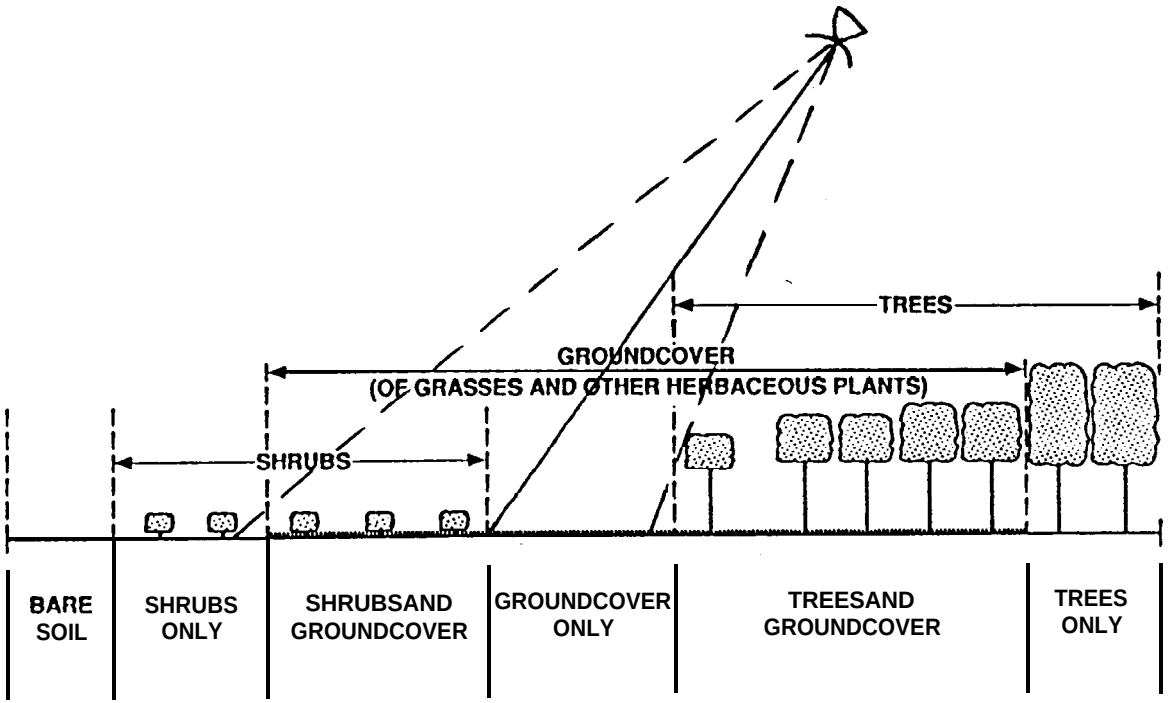

(T_a, τ_a)

(T_e, τ_c)

(T_e, r_{sp})

gure 2

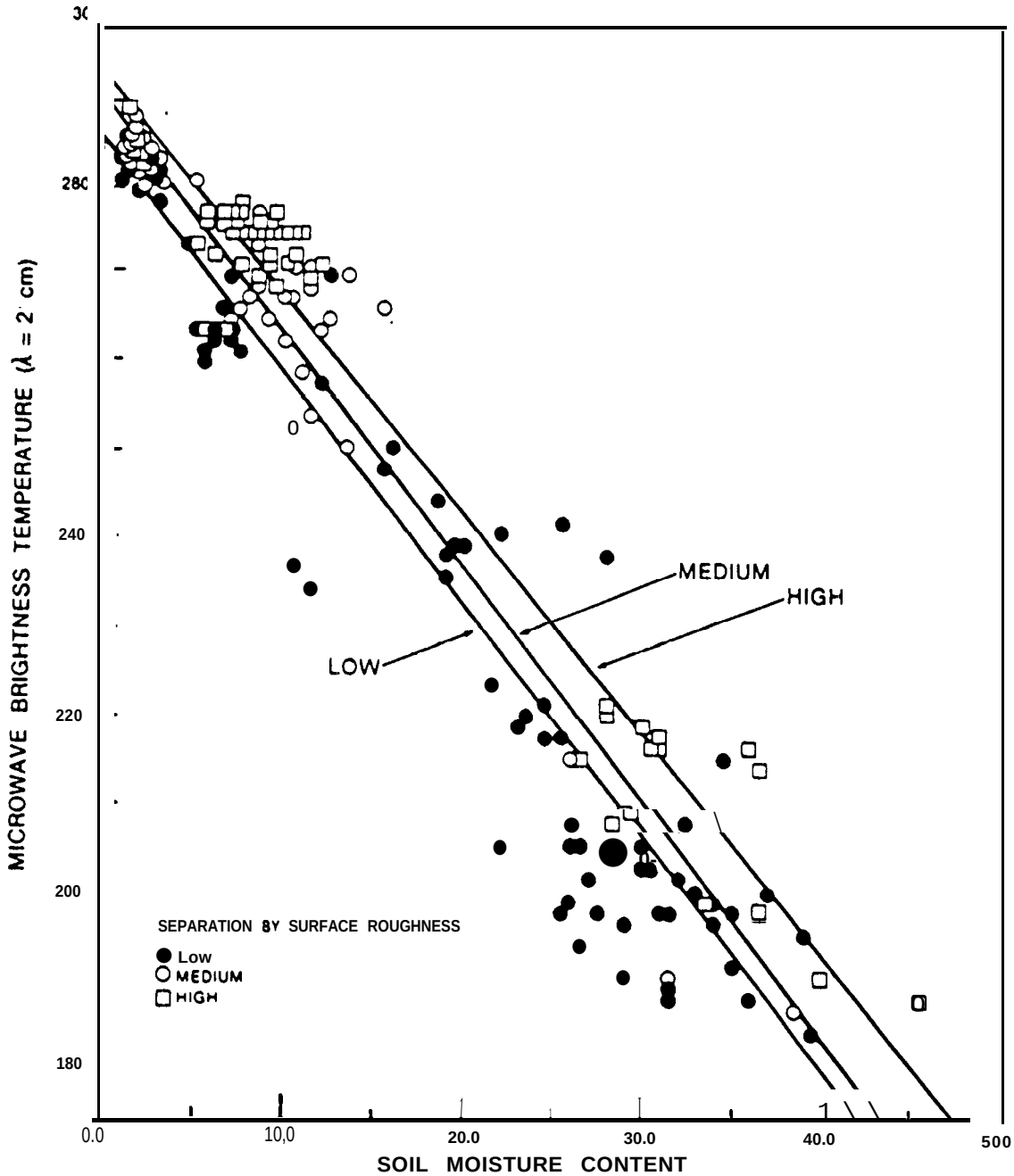
MICROWAVE BRIGHTNESS TEMPERATURE (λ = 2 cm)
280
240
220
200
180
MEDIUM
HIGH
LOW
SEPARATION BY SURFACE ROUGHNESS
Low
MEDIUM
HIGH
0.0
10,0
20.0
30.0
40.0
500
SOIL MOISTURE CONTENT

Figure 3

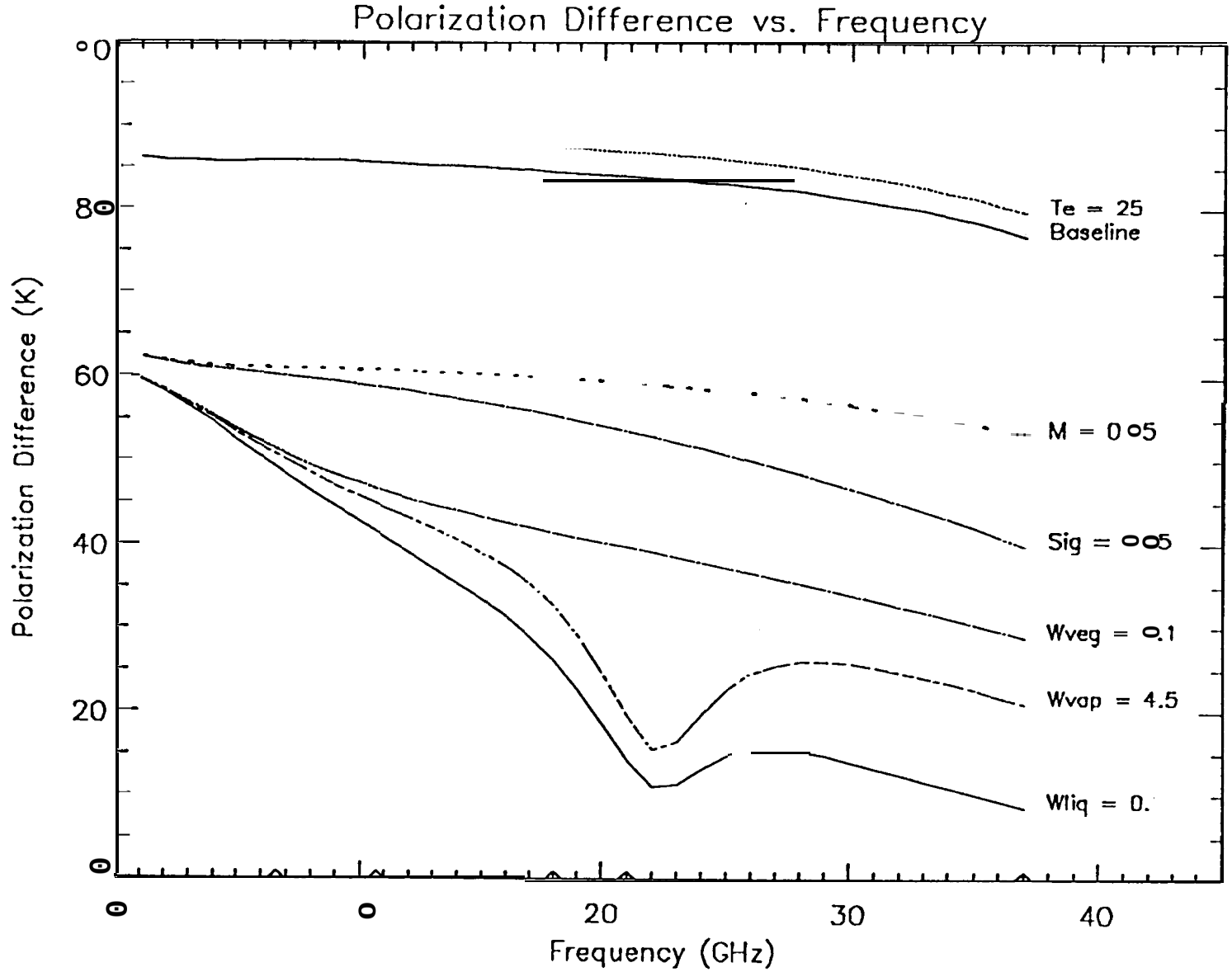
Polarization Difference vs. Frequency
Polarization Difference (K)
Frequency (GHz)
Te = 25
Baseline
M = 0 05
Sig = 005
Wveg = 0.1
Wvap = 4.5
Wliq = 0.
0
20
30
40
60
80

Figure 4

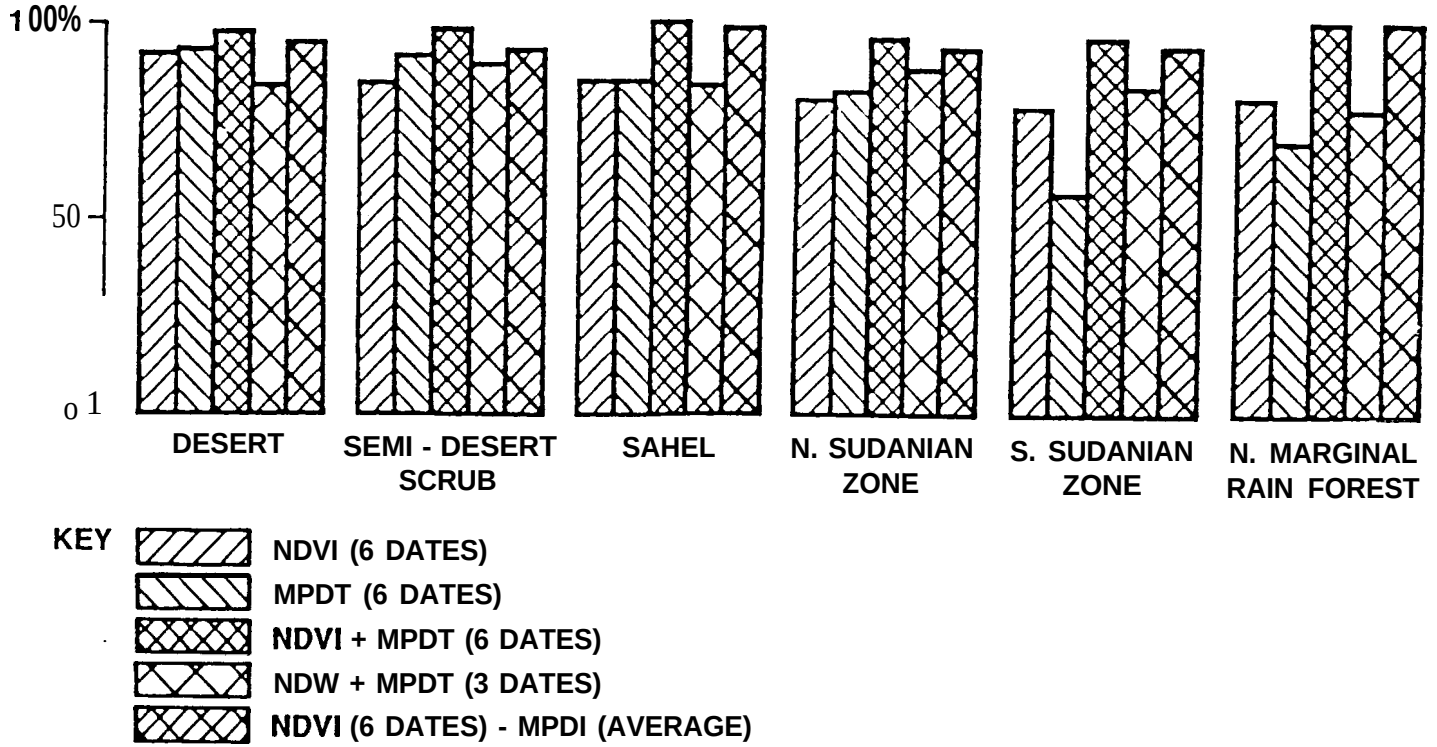
100%
50
0 1
DESERT
SEMI - DESERT SCRUB
SAHEL
N. SUDANIAN ZONE
S. SUDANIAN ZONE
N. MARGINAL RAIN FOREST
KEY
NDVI (6 DATES)
MPDT (6 DATES)
NDVI + MPDT (6 DATES)
NDW + MPDT (3 DATES)
NDVI (6 DATES) - MPDI (AVERAGE)

Figure 5

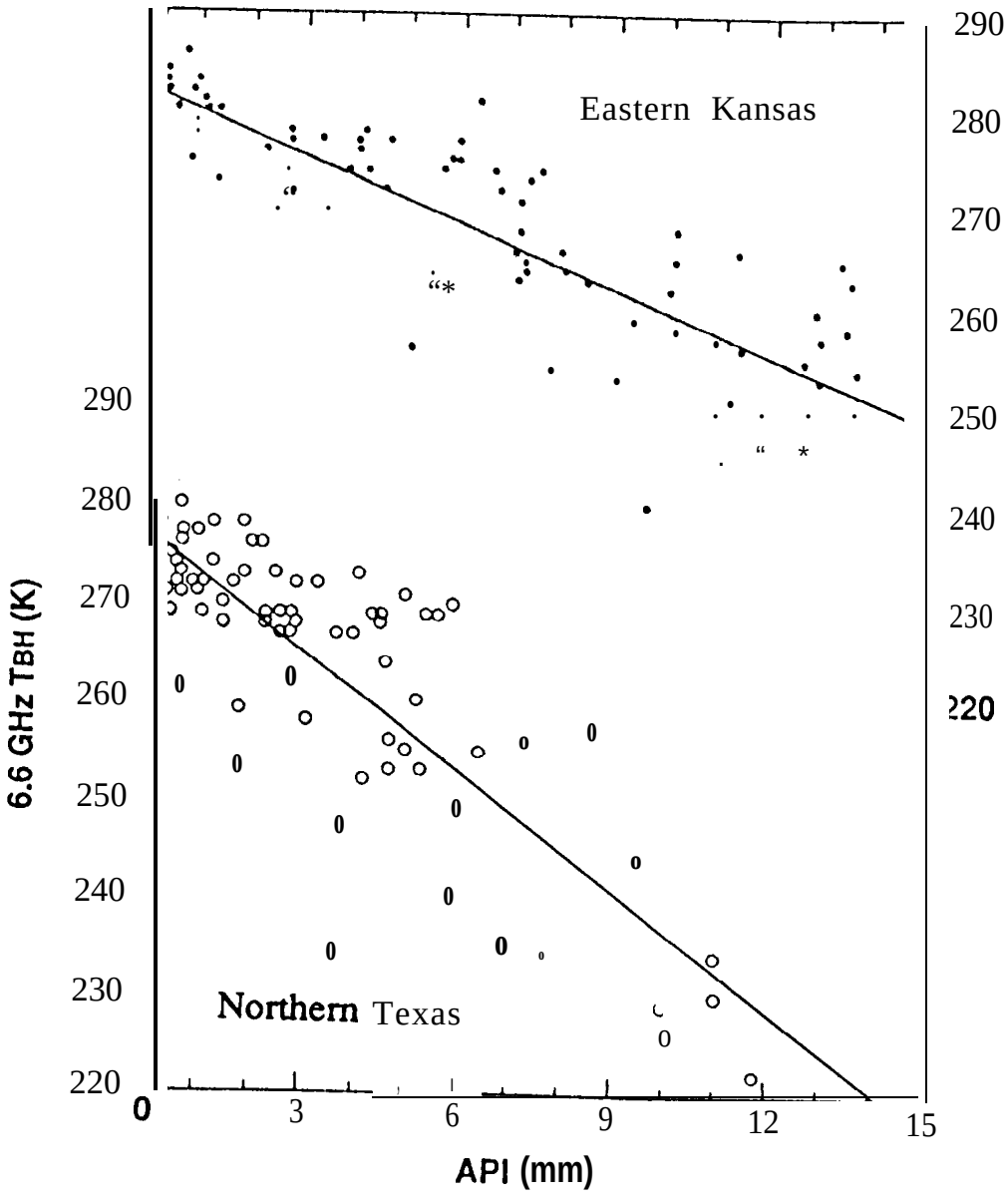
Eastern Kansas
Northern Texas
6.6 GHz TBH (K)
API (mm)
290
280
270
260
250
240
230
220
0
3
6
9
12
15

Figure 6

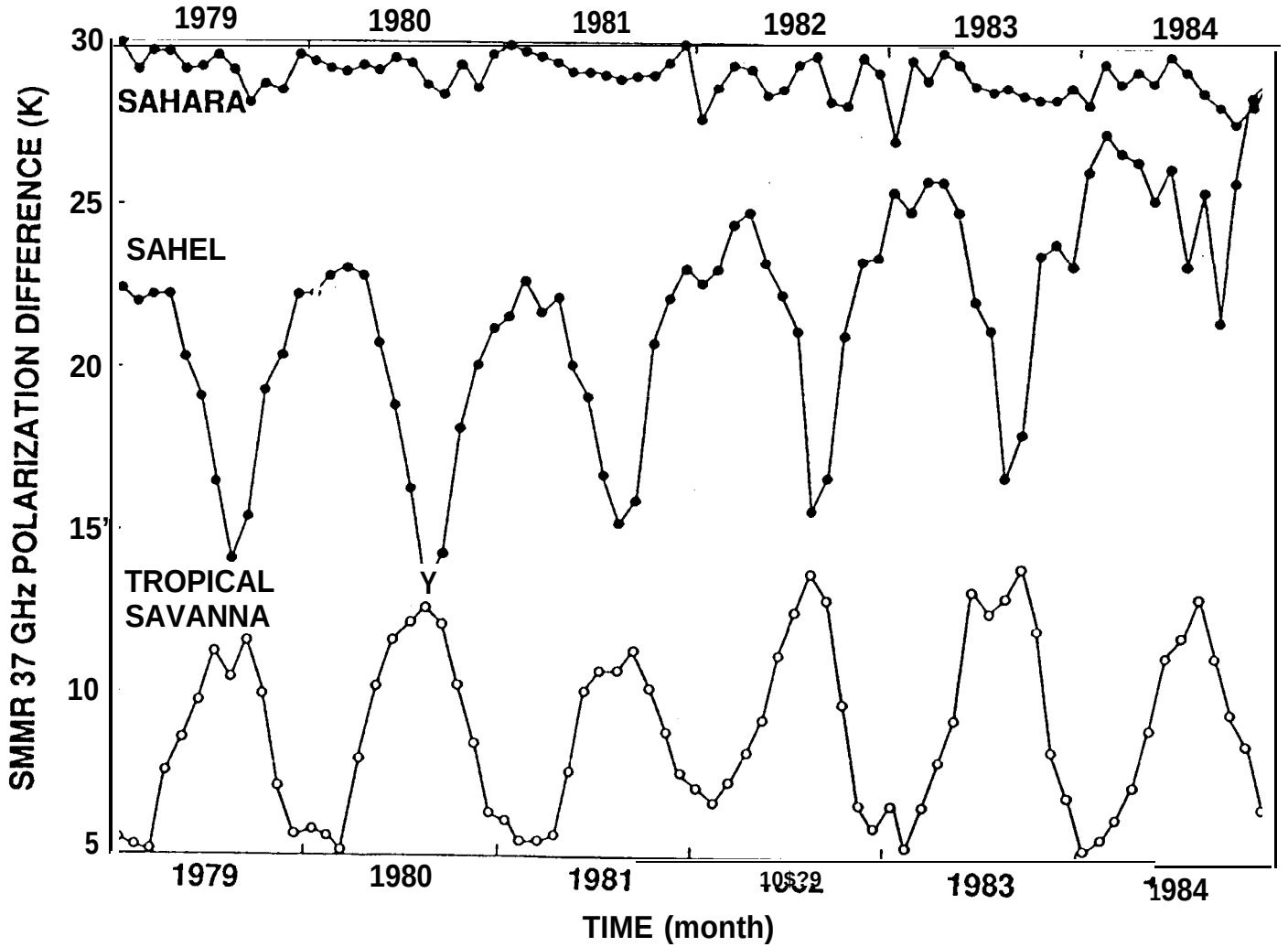
1979
1980
1981
1982
1983
1984
30
25
20
15
10
5
SAHARA
SAHEL
TROPICAL
SAVANNA
SMMR 37 GHz POLARIZATION DIFFERENCE (K)
TIME (month)

Figure 7

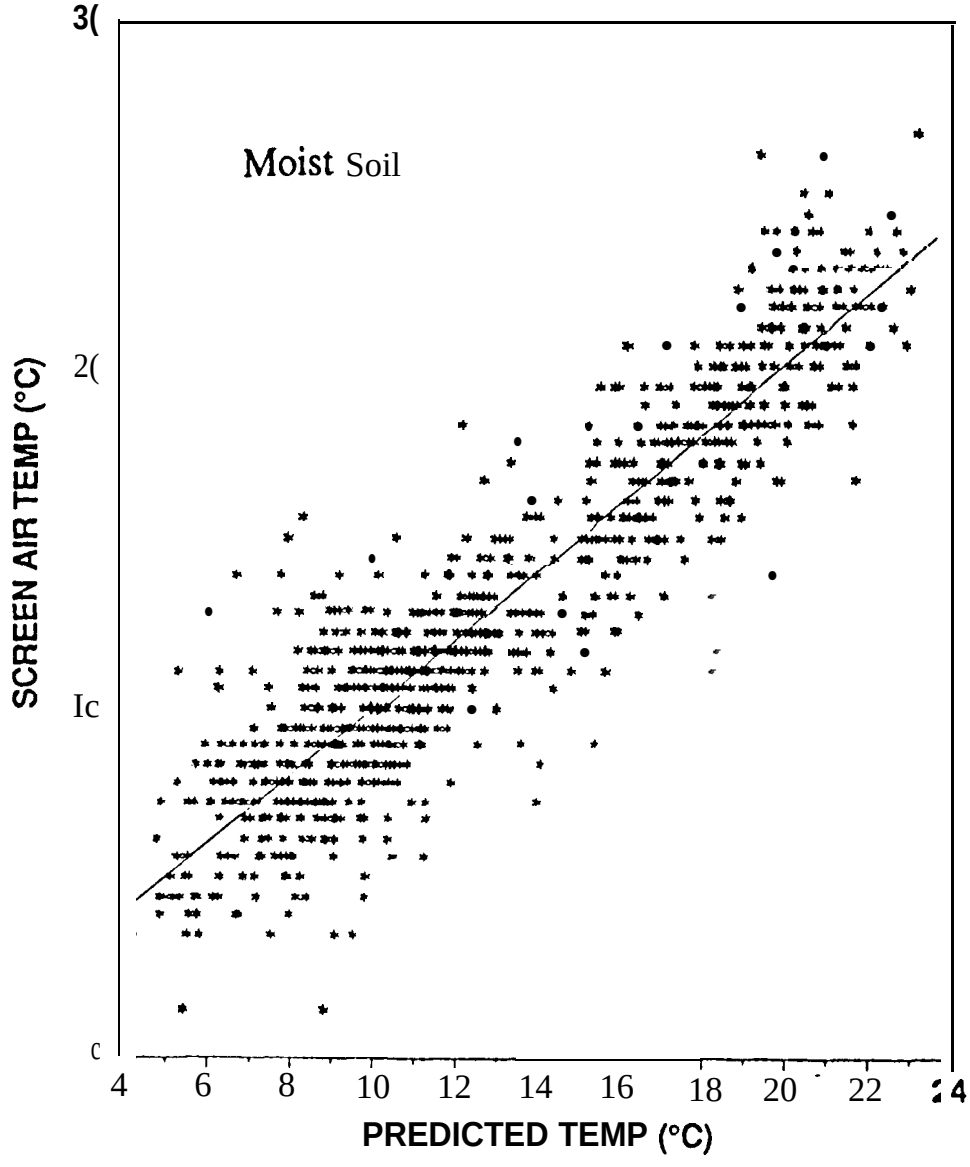

Regression Coefficients and Statistics for 4-Channel Model:

Land Surface Type	R^2	RMSE	Intercept	85 V	37 V	22 V	19 H
Crops/range	0.81	2.58	22.40	1.239	-0.396	0.275	-0.174
Moist soils	0.85	1.99	41.69	1,245	-0.724	0.415	**-0.063**
Dry soils	**0.62**	**2.60**	76.28	**-0.367**	**-0.318**	**1.408**	**0.025**
All	**0.79**	**2.37**	**58.07**	**0.811**	**-0.555**	**0.730**	**-0.170**

Figure 8